This article has been accepted for publication in a future issue of this journal, but has not been fully edited. Content may change prior to final publication. Citation information: DOI 10.1109/TIE.2014.2352214, IEEE Transactions on Industrial Electronics

Dynamic Performance Improvement of AC/DC Converter Using Model Predictive Direct Power Control with Finite Control Set

Dae-Keun Choi and Kyo-Beum Lee, *Senior Member, IEEE*

***Abstract*--This paper presents a control scheme for the dynamic performance improvement of an AC/DC converter using the model predictive direct power control (MPDPC) with duty cycle. In the MPDPC, the active and reactive powers are simultaneously controlled with a single cost function. If either of the two control targets has a large power variation, the control weight is concentrated on one side which causes the mutual interference. Because of such mutual interference, the control dynamics of the AC/DC converter deteriorates. Due to the control weight being concentrated on one side using the single cost function, even if the control dynamics of the other side decreases, the dynamic performance of the system is improved by reconfiguring the cost function that has the weighting factor to minimize the decline of the system dynamics which is caused by the mutual interference. The effectiveness of the proposed control scheme is verified by comparing its results with those of the conventional MPDPC. The results are obtained through the simulations and experiments.**

***Index Terms*--AC/DC power conversion, model predictive control (MPC), direct power control (DPC), converter control**

I. Introduction

Three-phase AC/DC converters have been extensively used in industrial application such as speed drives [1], renewable energies [2], active filters [3], [4], micro-grid systems [5], [6], and so on. Compared to a conventional diode rectifier, they have several advantages: bidirectional power flow, unity power factor and sinusoidal input AC current. Therefore, AC/DC converters are adopted in applications that require less distortion in the current waveforms for the purpose of observing the strict regulations on electrical harmonic pollutions. Since the AC/DC converter have abilities to control the input currents in sinusoidal waveforms, the unity power factor can be easily controlled by regulating the currents in phase with the grid voltages. Additionally, it has an advantage of reducing the size of the capacitor required by the system because the dc-link voltage is regulated by controlling the input power [7]-[14].

For the control methods of AC/DC converters, there are voltage oriented control (VOC) and direct power control (DPC) [15]-[18]. The VOC can indirectly control the input active and reactive powers by controlling the input current. Even though this method shows good dynamics and the stability of the steady state, it is affected by the performance of the internal current controller [19]. The DPC is another control method of AC/DC converters and is similar to the direct torque control (DTC) which is used for the motor drives. It calculates the active and reactive powers through the measurements of the input current and voltage, and instantaneously performs the power control by using the hysteresis comparator and the switching table. The voltage vector for the control is selected from a switching table which consists of the errors of active and reactive powers as well as the angular position of the estimated grid. Therefore, it does not need the internal current controller and shows excellent dynamics [20]-[22]. Since the switching table is set by considering the restricted control variables in the conventional DPC, the accuracy cannot be guaranteed in selecting the voltage vectors [23]. Hence, to improve the performance of the system, various methods, which enhance the performance of the DPC algorithm using the conventional switching table, have been proposed such as reorganizing the conventional switching table [24], using the fuzzy control, and etc [25].

Recently, a model predictive direct power control (MPDPC) algorithm that incorporates the conventional DPC algorithm to the model predictive control algorithm has been proposed. Even though the control method of the MPDPC is similar to the conventional DPC, the MPDPC predicts, based on the system model, the future state to select the optimal voltage vector which is different from the method that selects the vector from the switching table [26]-[31]. Based on the model, the cost function consists of the errors of the active and reactive powers to evaluate the effect of each voltage vector and selects the optimal voltage vector [32]-[41]. Because the voltage vector is selected by predicting the next state, it is more accurate and effective compared to the DPC method that

Manuscript received November 9, 2013; revised February 19, 2014, April 2, 2014, and May 19, 2014; accepted June 18, 2014.

This work was supported by the Human Resources Development program (No. 20134030200310) of the Korea Institute of Energy Technology Evaluation and Planning (KETEP) grant funded by the Korea government Ministry of Knowledge Economy.

This research was supported by Basic Science Research Program through the National Research Foundation of Korea(NRF) funded by the Ministry of Education (2013R1A1A2A10006090)

Dae-Keun Choi and K. B. Lee are with the Department of Electrical and Computer Engineering, Ajou University, Suwon, 443-749, Korea (e-mail: bigbig80@ajou.ac.kr, kyl@ajou.ac.kr).

This article has been accepted for publication in a future issue of this journal, but has not been fully edited. Content may change prior to final publication. Citation information: DOI 10.1109/TIE.2014.2352214, IEEE Transactions on Industrial Electronics

selects the voltage vector using the switching table [42]-[45].

The MPDPC can achieve a good steady state performance and quick dynamic response by selecting the optimal voltage vector, which minimizes the error between the reference power and the actual power. The optimal voltage vector is determined by the control scheme that minimizes the cost function. The cost function used in the MPC for the power control generally consists of the sum of the square or absolute values from the error term of the active and reactive powers and is used to find an appropriate control input from the finite input set. When using the cost function that consists of absolute value, it can have balanced control because of small mutual interference between active and reactive powers. When using the cost function consisting of square terms, the dynamics may increase but mutual interference can be occurred during active and reactive power control [42]-[44].

In the MPDPC with duty cycle in [44], the two control factors, which are the active and reactive powers, are composed into a single cost function and are controlled simultaneously. In this paper, the MPDPC method selects the voltage vector for the system control using the cost function according to the error amount of active and reactive powers, calculates the effective time of the selected voltage vector, and applies the selected voltage vector to the system. Since a cost function consists of the sum of the two square terms of the errors from the active and reactive powers, these two powers cannot be independently controlled from each other, thus each of the control of active and reactive powers causes influence to one another. As the mutual influence becomes larger as the variation amount of the active and reactive powers becomes larger, the mutual interference will increase during the control. At this moment, the response characteristic will decrease causing the negative influence to the control. If either of the two control targets (active and reactive powers) has a large power variation, the control weight is concentrated on one side, causing the mutual interference. If the variation of the power becomes larger, the mutual interference becomes even more larger. Due to such mutual interference, the control dynamics of the AC/DC PWM converter deteriorates.

Such mutual interference generates voltage ripple due to swell or sag in the output voltage of the transient state during the output voltage control of the ac/dc converter and causes the distortion of the output voltage waveform.

Additionally, in the case of the load system with severe change of the power usage pattern, the decrease of the output voltage control characteristic generated by the mutual interference component in the transient-state interval becomes even larger. Such distortion of the output voltage due to the decrease of the control characteristic imposes more stress to the load system and decreases the performance of the efficiency and operation of the load system.

In this paper, the control scheme for the dynamic performance improvement is proposed for an AC/DC converter using the MPDPC. The cost function in [44] is reorganized to solve the generated mutual interference problem by using the single cost. Using the reconfigured cost function, the mutual interference has been reduced and the dynamic performance of the system is improved. The effectiveness of the proposed control scheme is verified by results obtained through simulations and experiments.

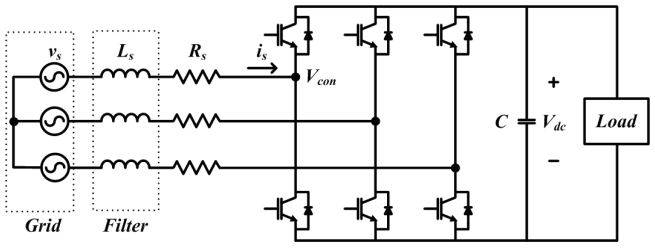

Fig. 1. Topology of the three-phase AC/DC converter.

II. Predictive Model of AC/DC PWM Converter

The topology of the three-phase AC/DC PWM converter is shown in Fig. 1. It is composed of a three-phase full bridge converter with six power transistors which are connected to the grid voltage v_s through the filter inductance L_s and resistance R_s. The model of the AC/DC PWM converter can be defined in the stationary frame as follows:

$$v_s = L_s \frac{di_s}{dt} + R_s i_s + v_{con} \tag{1}$$

where v_s is the grid voltage vector, v_{con} is the output voltage vector of the converter, i_s is the input current vector. The output voltage vector of converter is calculated from the switching state and dc-link voltage, and can be written as

$$v_{con} = s_{con} V_{dc} \tag{2}$$

where V_{dc} is the dc-link voltage and s_{con} is the switching state vector of the PWM converter. Switches s_a, s_b, and s_c show the switching state of each leg, where 1 represents ON and 0 represents OFF.

$$s_{con} = \frac{2}{3}(s_a + s_b e^{j2\pi/3} + s_b e^{-j2\pi/3}) . \tag{3}$$

The complex power S can be calculated from the grid voltage and current vectors as

$$S = p + jq = \frac{3}{2}(i_s^* v_s) \tag{4}$$

where p is the active power, q is the reactive power and "*" is the conjugate operator. If three phases of the grid voltage are balanced, the differentiation of the grid voltage v_s can be defined as

$$\frac{dv_s}{dt} = j\omega \mid v_s \mid v_s^{j\omega t} = j\omega v_s \tag{5}$$

where ω is the grid frequency. From (1), the differentiation of the grid current can be obtained as

This article has been accepted for publication in a future issue of this journal, but has not been fully edited. Content may change prior to final publication. Citation information: DOI 10.1109/TIE.2014.2352214, IEEE Transactions on Industrial Electronics

$$\frac{di_s}{dt} = \frac{1}{L_s}(v_s - v_{con} - R_s i_s)\,. \tag{6}$$

Substituting (5) and (6) into (4), the differentiation of the complex power S can be obtained as

$$\frac{dS}{dt} = \frac{1}{L_s}\left[\frac{3}{2}\left(|\,v_s\,|^2 - v_{con}^* v_s\right) - (R_s - j\omega L_s)S\right]. \tag{7}$$

Separating the differentiation of the complex power S in (7) into the real part and the imaginary part, the differentiation of the active and reactive powers are obtained as

$$\frac{dp}{dt} = \frac{3}{2L_s}\left[|\,v_s\,|^2 - \mathrm{Re}(v_{con}^* v_s)\right] - \frac{R_s}{L_s}p - \omega q \tag{8}$$

$$\frac{dq}{dt} = \frac{-3}{2L_s}\mathrm{Im}(v_{con}^* v_s) - \frac{R_s}{L_s}q + \omega q\,. \tag{9}$$

Using the active and reactive powers from (8) and (9), the prediction value of p and q at the next control period can be obtained as [44]

$$p^{k+1} = p^k + \left(\frac{3}{2L_s}\left[|\,v_s^k\,|^2 - \mathrm{Re}\left(\left(v_{con}^k\right)^*\left(v_s^k\right)\right)\right]\right)t_{sp} - \left(\frac{R_s}{L_s}p^k + \omega q^k\right)t_{sp} \tag{10}$$

$$q^{k+1} = q^k + \left(\frac{-3}{2L_s}\mathrm{Im}\left(\left(v_{con}^k\right)^*\left(v_s^k\right)\right) - \frac{R_s}{L_s}q^k - \omega q^k\right)t_{sp}\,. \tag{11}$$

When using the control based on the power prediction equations (10) and (11) of the actual system control, the one step delay problem is generated. Such a delay problem causes an error on the power prediction for the control. To resolve such a delay problem, the (k+2)th power prediction value that is acquired through the model is used for the control instead of (k+1)th. The (k+1)th value is obtained from (10) and (11) using the output voltage of the selected converter from the previous sampling time, and the related (k+2)th active and reactive power equation can be expressed using the applicable (k+1)th converter output voltage as follows:

$$p^{k+2} = p^{k+1} + \left(\frac{3}{2L_s}\left[|\,v_s^{k+1}\,|^2 - \mathrm{Re}\left(\left(v_{con}^{k+1}\right)^*\left(v_s^{k+1}\right)\right)\right]\right)t_{sp} - \left(\frac{R_s}{L_s}p^{k+1} + \omega q^{k+1}\right)t_{sp} \tag{12}$$

$$q^{k+2} = q^{k+1} + \left(\frac{-3}{2L_s}\mathrm{Im}\left(\left(v_{con}^{k+1}\right)^*\left(v_s^{k+1}\right)\right)\right)t_{sp} - \left(\frac{R_s}{L_s}q^{k+1} - \omega q^{k+1}\right)t_{sp}. \tag{13}$$

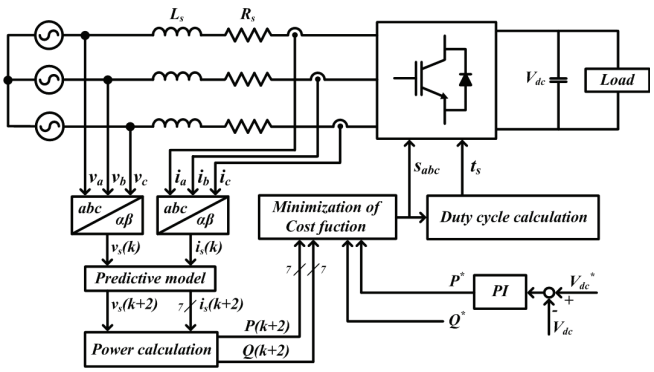

Fig. 2. Block diagram of the MPDPC for the AC/DC converter.

III. MPDPC Control Scheme for Dynamic Performance Improvement

In the conventional MPDPC in [44], the two control factors, the active and reactive powers, are composed into the single cost function and are controlled simultaneously. If the power control is performed using the single cost function without weighting factor in the small scale system, the mutual interference is small. If the power changes drastically in a large scale system which uses the single cost function without weighting factor, the control weight is concentrated on either active or reactive power and the dynamic performance on the other target deteriorates.

In this paper, the optimized voltage vector is selected for the control of active and reactive power by using the reorganized cost function to enhance the reduced dynamic performance of the system which is generated when implementing the single cost function without weighting factor in a large scale system. When the proposed method is applied, the mutual interference, which is generated by using the single cost function without weighting factor, is reduced.

A. Optimal vector selection using reconfigured cost function

The main purpose of the cost function is tracking a particular variable for the control of the system. It has other advantages as well. One of the main features of the MPC is that any required term which could be a variable, constraint or requirement of the system for a prediction is used for the cost function. This feature allows the MPC to gain the control more easily which results in several benefits such as better efficiency, safety, power quality. There is possibility that these terms can be different factors which makes the system more difficult to control because of coupling effects between two factors or placing more weight on one factor compare to other factors, which diminishes the influence of other factors or even make them uncontrollable. To avoid such situations, the weighting factors are included in each term of the cost functions used by the MPC. By adjusting such weighting factors, the system performance can be improved or adjusted.

The cost function used in the MPC for the power control generally consists of the sum of the square or absolute values from the error term of the active and reactive powers and is

This article has been accepted for publication in a future issue of this journal, but has not been fully edited. Content may change prior to final publication. Citation information: DOI 10.1109/TIE.2014.2352214, IEEE Transactions on Industrial Electronics

used to find an appropriate control input from the finite input set. The cost function used in this paper is composed of the square terms of the active power error and reactive power error as shown in (14) and is used to select a voltage vector appropriate for the control. Next, the effective time of the selected vector is calculated in order to minimize the power ripple and applied to the system. The cost function selects the voltage vector that minimizes the sum of the square term of the active power error and the square term of the reactive power error. During this control process, if the difference between the active power error and the reactive power error is not large, the control can be performed without an additional weighting factor due to the same nature of the active power and the reactive power. Since the difference between the active power error and the reactive power error is not large in the small rated power system, it is less affected by the mutual interference. However, in such a case where either of the active power error or the reactive power error changes drastically in the large rated power system, it selects the control input concentrated to one-side because a large difference between the errors from both sides is produced.

In this paper, since the cost function of the square form is used in order to calculate the duty cycle of the selected vector in the finite input set, the error difference from both sides becomes even larger. As a result, the mutual interference that does not occur in the small rated power system is generated in the large rated power system. The contents mentioned above are explained in detail in latter part of Section III-A. When the conventional MPDPC in the small scale systems is used to control the power, the dynamic performance is still guaranteed because of small mutual interference even though the active and reactive powers are controlled with a conventional single cost function.

However, in the case of the system with large scale, since one of the error components from both active and reactive powers, which compose the cost function, increases drastically, the dynamic performance of the other side decreases. To improve the dynamic performance of the conventional MPDPC, the cost function which is used for selecting the optimal voltage vector in the MPDPC is reorganized. By using the reconfigured cost function, the dynamic performance of the system can be improved even when the mutual interference occurs. The weighting factor is included to minimize the mutual interference in the single cost function.

The weighting factor for the error term of the active power can adjust its magnitude according to the magnitude of the error term of the reactive power. On the other hand, the weighting factor for the error term of the reactive power can adjust its magnitude according to the magnitude of the error term of the active power. By adding this weighting factor, the mutual interference, which is generated when both the active and reactive powers are simultaneously controlled by using the conventional cost function in a large scale system, can be minimized. The reconfigured cost function can be expressed as

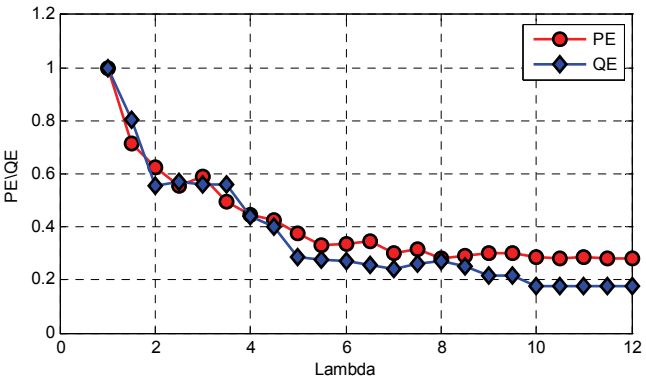

Fig. 3. The variation of mutual interference according to the λ (lamda) value.

$$cf_{recon} = p_{wf}(p^{ref} - p^{k+2})^2 + q_{wf}(q^{ref} - q^{k+2})^2 . \quad (14)$$

where cf_{recon} is cost function. The added weighting factors for the reconfigured cost function can be organized as

$$p_{wf} = \left[\lambda \left| \left(q^{ref} - q^{k+2} \right) / q_{rated} \right| + 1 \right] \quad (15)$$

$$q_{wf} = \left[\lambda \left| \left(p^{ref} - p^{k+2} \right) / p_{rated} \right| + 1 \right] \quad (16)$$

where p_{wf} and q_{wf} are the weighting factor for the dynamic performance compensation, p^{ref} is the reference of the active power, q^{ref} is the reference of the reactive power, p_{rated} is the rated value of active power, q_{rated} is the rated value of reactive power. The constant value of one is added to the value of the power error divided by the rated power to prevent the cost function from becoming zero when the power error becomes zero. For the situation where the active power changes drastically, the value of q_{wf} increases more rapidly compared to p_{wf} compensating the dynamic performance of the reactive power; on the contrary, for the situation where the reactive power changes drastically, the value of p_{wf} increases more rapidly compared to q_{wf} compensating the dynamic performance of the active power. λ is scaling factor for adjusting the amount of the weighting factor. By adjusting the value of λ, the dynamic performance appropriate for the system can be obtained.

$$p_{merr} = p^{ref} - p_m \quad (17)$$

$$q_{merr} = q^{ref} - q_m \quad (18)$$

where p_m is the magnitude of the generated mutual interference component in the active power, q_m is the magnitude of the generated mutual interference component in the reactive power, p_{merr} is the error of the active power component generated by the mutual interference, and q_{merr} is the error of the reactive power component generated by the mutual interference.

PE is the amount of mutual interference generated to active power due to the change of reactive power, while *QE* is the value generated to the reactive power due to the change of

This article has been accepted for publication in a future issue of this journal, but has not been fully edited. Content may change prior to final publication. Citation information: DOI 10.1109/TIE.2014.2352214, IEEE Transactions on Industrial Electronics

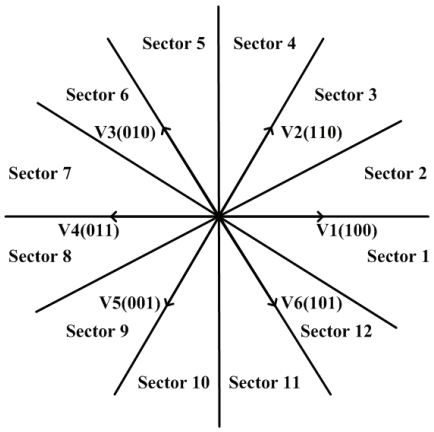

Fig. 4. Sectors in stationary coordinates and converter voltage vectors.

the active power. Both of them are normalized values. It can be expressed as

$$PE = \frac{p_{merr}}{p_{merr\_\max}} \tag{19}$$

$$QE = \frac{q_{merr}}{q_{merr\_\max}} \tag{20}$$

where $p_{merr\_\max}$ is the maximum value of (17) and $q_{merr\_\max}$ is the maximum value of (18).

Fig. 3 shows the reduced amount of mutual interference according to the value of λ (Lambda). The normalized value of the error generated by the mutual interference in the active power and the reactive powers as the value of λ changes is expressed in the graph. The size of decreasing mutual interference appears almost identical above 10, and it can be verified that the size of the mutual interference is constant above 12 but the steady state control performance is decreased above 12. Hence, the λ value is set to 11 so that the size of mutual interference is minimized while maintaining the steady state performance. The value of λ is the determined optimal value based on the simulations and experiments and the optimal value of λ can be adjusted according to the system parameters. In the case of the system parameters have modification (especially concerning the inductance value of the filter), it is desirable to optimize through customization to the system by adjusting the lambda value for the system control performance.

To select the optimal voltage vector for the power control, the reconfigured cost function of (14) is used. There are eight possible voltage vectors in the two-level inverter and, for the selection of the optimal vector, the vector that minimizes the cost function is selected among the eight voltage vectors. Using (12) and (13), the powers of the next period for each of eight usable vectors are predicted and the optimal vector is selected by finding the minimized value from (14). In this paper, both active and zero vectors are used together during one control period after calculating the optimized duty cycle for active vector. However, if the vector that minimizes the

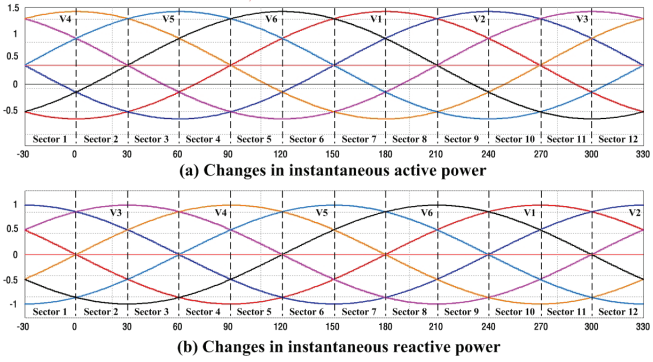

Fig. 5. Instantaneous change of the active and reactive power corresponding to the voltage vectors of the converters.

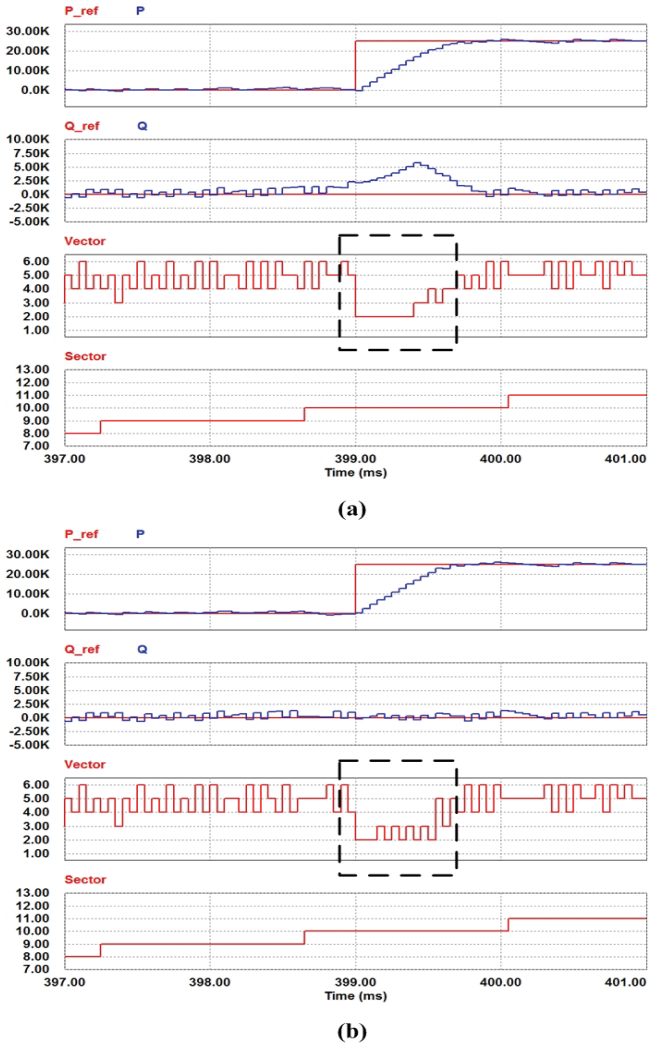

Fig. 6. Comparing the change of the voltage vector selected for the power control when using the conventional cost function and the proposed cost function.

cost function is the zero vector, the second best vector has to be selected rather than the zero vector. Active vector is necessary to be evaluated for the cost function, since the zero vector has been selected as one of the two vectors for the

This article has been accepted for publication in a future issue of this journal, but has not been fully edited. Content may change prior to final publication. Citation information: DOI 10.1109/TIE.2014.2352214, IEEE Transactions on Industrial Electronics

MPDPC with duty cycle. In this case, the combination of second best vector (active vector) and best vector (zero vector) satisfies the cost function (14) better than that of using zero vector only. The duty cycle of the active vector is calculated in Section III-B.

For verification of the performance of reconfigured cost function with weighting factor, the change of the voltage vector selected for the power control is analyzed when using the conventional cost function and the proposed cost function. For this analysis, the phase of the power-source voltage vector is converted to the digitized signal sector n. The stationary coordinates are divided into 12 sectors, and V indicates the voltage vector of the converter as shown in Fig. 4. Fig. 5 shows the plots of the instantaneous change of the active and reactive power corresponding to each sector of the voltage source for all the voltage vectors of the converters. Fig. 6 show, from the top, the active power, reactive power, the voltage vectors selected by the cost function, and the angular position of the grid voltage

In Fig. 6, the reference value of the active power is changed to 25 kW at 0.399 s and the reactive power is controlled at 0. In the interval where the reference power increases, the angular position of the grid voltage is located in sector 10. In Fig. 6(a), only the voltage vector 2 is applied to the interval where the power increases; as a result, it can be verified that the mutual interference is generated to the reactive power which is controlled as 0. In the case of the voltage vector 2 being applied to sector 10, the active power increase the most, but reactive power also increases as well. Thus, if only the voltage vector 2 is continually applied in the interval where the reference active power increases, the reactive power also increases. Fig. 6(b) is the case when the cost function with the added weighting factor considered by the changing amount of the power error is applied. Unlike the previous case which uses the conventional cost function from Fig. 6(a), in the interval where the power is increased, the voltage vectors 2 and 3 are used together. The voltage vector 3 in sector 10 increases the active power and the reactive power decreases at the same time. Hence, in the interval where the active power increases by using both the voltage vectors 2 and 3, the mutual interference can be compensated. In the case of using the reconfigured cost function, the error of the reactive power generated by the mutual interference minimizes.

However, the response delay may occur when using the reconfigured cost function since both voltage number 2 and 3 are used for the mutual interference compensation instead of using only voltage vector 2, which makes the largest contribution, when tracking active power reference. However, the system control and response time are not largely affected even though the speed may slightly decrease as shown in Fig. 6.

B. Calculation of duty cycle for voltage vector

In this paper, the MPDPC uses the duty cycle control to achieve the better performance than that of the conventional single-vector-based MPDPC. The control period is divided into two sectors: one for the active vector selected from minimizing the cost function and the other for the zero vector. The duration of the selected active vector is derived based on the principle of the power error minimization [44]. After selecting the optimal active voltage vector using (14), the duration of the active vector is calculated. s_{p1} and s_{p2} are the slopes of the active power when the active and zero vectors are applied and s_{q1} and s_{q2} are the slopes of the reactive power when the active and zero vectors are applied. They can be calculated by using (12) and (13). The values of active and reactive powers are obtained as follows:

$$p^{k+2} = p^{k+1} + s_{p1} \cdot t_s + s_{p2} \cdot (t_{sp} - t_s) \tag{21}$$

$$q^{k+2} = q^{k+1} + s_{q1} \cdot t_s + s_{q2} \cdot (t_{sp} - t_s) \tag{22}$$

where t_s is the duration of the active vector and t_{sp} is the control period. The optimal duration of t_s during a control period satisfies the following condition:

$$\frac{\partial cf_{recon}}{\partial t_s} = 0 . \tag{23}$$

The duty cycle of the active vector can be obtained by using (23) as follows:

$$t_s = \frac{(p^{ref} - p^{k+2})(s_{p1} - s_{p2}) + (q^{ref} - q^{k+2})(s_{q1} - s_{q2})}{(s_{p1} - s_{p2})^2 + (s_{q1} - s_{q2})^2} + \frac{t_{sp}(s_{p2}^2 + s_{q2}^2 - s_{p1}s_{p2} - s_{q1}s_{q2})}{(s_{p1} - s_{p2})^2 + (s_{q1} - s_{q2})^2} \tag{24}$$

The active vector is applied during t_s, which is acquired by using (24), and a zero vector is applied during the remaining time, where t_s is subtracted from a control period t_{sp}. If t_s is smaller than zero, ts should be limited to zero; on the other hand, if t_s is larger than t_{sp}, t_s is should be limited to t_{sp}.

TABLE I
PARAMETERS FOR SIMULATION

Grid voltage (line-to-line)	380 Vac [rms]
DC-link voltage	700 Vdc
DC-link capacitor	3300 uF
Rated power	25 kW
Filter inductance	8 mH
Switching frequency	20 kHz

IV. SIMULATION RESULTS

In order to verify the validity of the proposed algorithm, a simulation was performed using PSIM. The simulation was carried out under the conditions listed in Table I. The simulation circuit of the AC/DC PWM converter is the same as Fig. 1. The MPDPC method is explained in the block diagram of Fig. 2. To compare the performance of the

This article has been accepted for publication in a future issue of this journal, but has not been fully edited. Content may change prior to final publication. Citation information: DOI 10.1109/TIE.2014.2352214, IEEE Transactions on Industrial Electronics

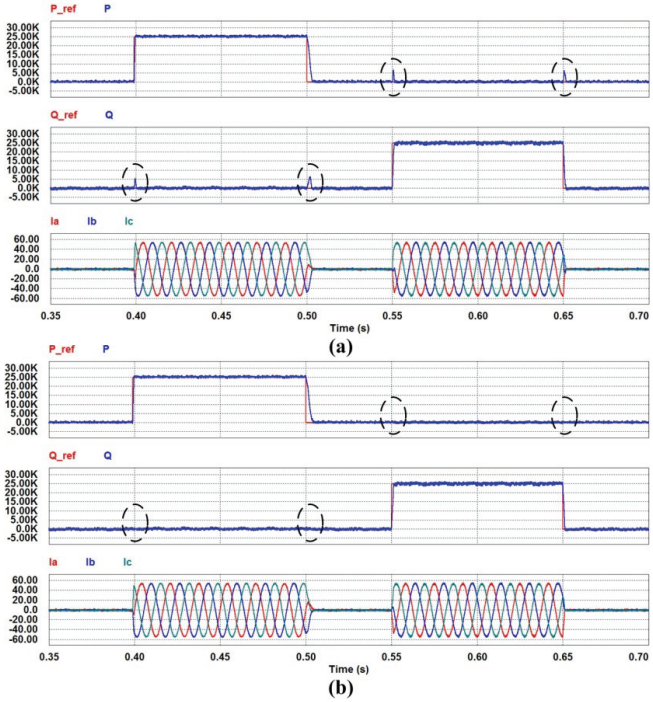

Fig. 7. Simulation results of power step responses.
(a) Conventional MPDPC. (b) Proposed MPDPC.

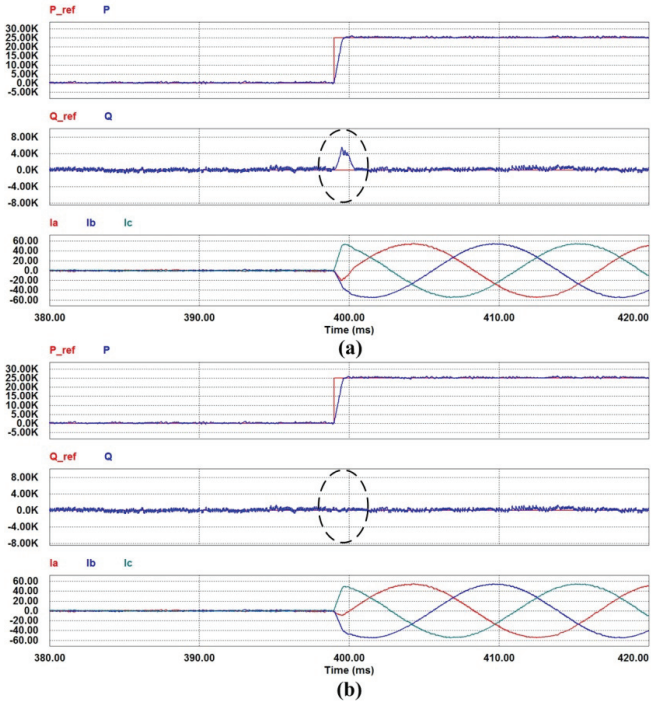

Fig. 8. Waveforms in expanded views in Fig. 7 (from 380 ms to 420 ms).
(a) Conventional MPDPC. (b) Proposed MPDPC

proposed method with the conventional MPDPC, the simulation configurations are under exactly the same condition. The duty cycle calculation is applied to both the conventional MPDPC method and the proposed MPDPC method. The compensation waveforms between the proposed and conventional methods are both performed under the same switching frequency of 20 kHz.

The following simulation results are the waveforms when the MPDPC is performed using the reconfigured cost function. Fig. 7 is the simulation waveforms that compare the step response of the conventional MPDPC with the proposed MPDPC. The reference of the active power is increased to 25 kW and decreased to 0 kW. Then, the reference of the reactive power is increased to 25 kVar and decreased to 0 kVar. From the top, it shows the active power, reactive power, and grid current. Under step-change conditions of the power reference, the sector where the mutual interference occurs is marked in dashed circles. Fig. 7(a) shows the waveform when the MPDPC is performed using the conventional cost function. In section where the reference of the active power changes, it shows that the mutual interference occurs in the reactive power. Likewise, in section where the reference of the reactive power changes, it shows that the mutual interference occurs in the active power. By minimizing such mutual interference, to improve the dynamic performance of the converter, the MPDPC is performed through the reconfigured cost function. Fig. 7(b) shows the waveform when the MPDPC is performed using the reconfigured cost function. By comparing the sections marked with the dashed circles of Fig. 7(a) and Fig. 7(b), it can be verified that the unstable parts which is caused by the mutual interference is minimized.

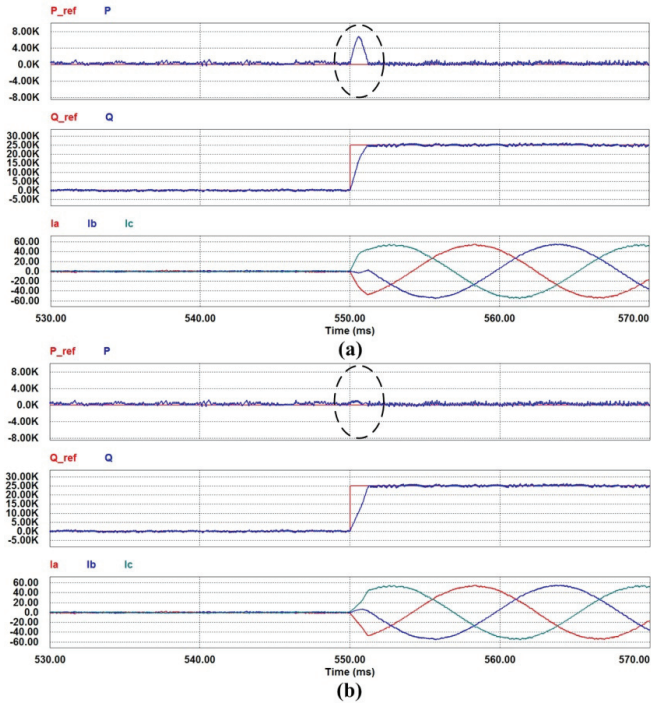

Fig. 9. Waveforms in expanded views in Fig. 7 (from 530 ms to 570 ms).
(a) Conventional MPDPC. (b) Proposed MPDPC

Figs. 8 and 9 show the expanded view of sections where mutual interference is generated in Fig. 7. It can be validated that the dynamic performance is improved in the sector where the power changes by observing that the mutual interference generated in section, where the reference of the active power

This article has been accepted for publication in a future issue of this journal, but has not been fully edited. Content may change prior to final publication. Citation information: DOI 10.1109/TIE.2014.2352214, IEEE Transactions on Industrial Electronics

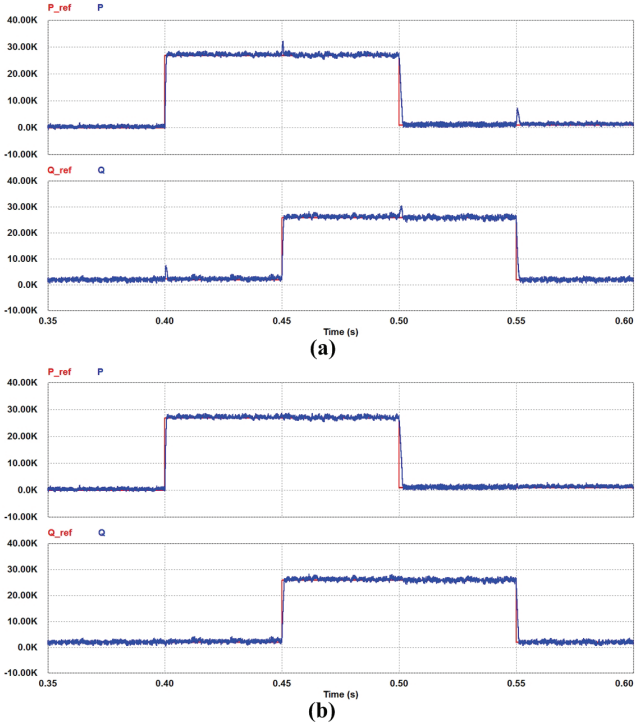

Fig. 10. Simulation results under conditions of step changes in active and reactive power references
(a) Conventional MPDPC. (b) Proposed MPDPC.

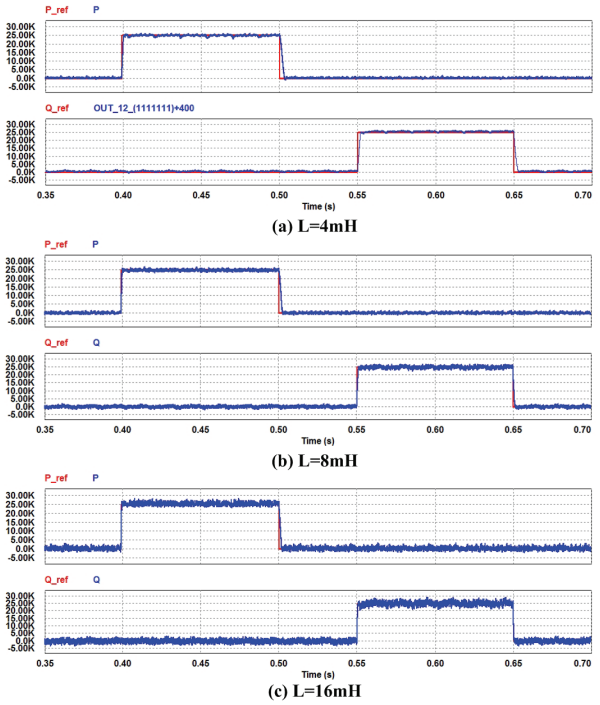

Fig. 11. Verification of system robustness in the case of inductance in control differs from real value.

rises to 25 kW in Fig. 8(a), is eliminated in Fig. 8(b). Like changing the active power, Fig. 9(a) presents that dynamic performance of the active power control is decreased due to the mutual interference in section, where the reference of the reactive power rises to 25 kVar in Fig. 9(a). When performing the MPDPC using the reconfigured cost function, it can be confirmed that the dynamic performance is enhanced in the sector where the mutual interference occurs as shown in the waveform of Fig. 9(b). In the case when the conventional cost function is used through the simulation, the weighting factor can be concentrated to one side and it is confirmed that the mutual interference is generated at this moment. To resolve this problem, the proposed MPDPC method is applied and, as a result, the mutual interference is eliminated leading to the improvement in the dynamic performance of the control.

In the case of using the reconfigured cost function, it can be verified through the simulation waveform, as shown in Fig. 8(b), that the control is performed well tracking the given active power reference, and the response time is almost 1 ms which verifies to be almost identical to the response time using the conventional cost function in Fig. 8(a). When changing the reactive power reference value in Fig. 9(b), the system operates well according to the reference value as if changing the active power reference value in Fig 8(b). However, it can be verified that the response speed from Fig. 9(b), which uses the reconfigured cost function, is slower than the one from Fig. 9(a), which uses the conventional cost function. When using the reconfigured cost function, the response speed may become slower since the vector, that tracks the reference value of the control target and simultaneously minimizes the mutual interference component generated in other control target, is selected. However, it does not largely affect the control performance and can verify that the response times are almost identical.

Fig. 10 shows the simulation waveform when varying the reference value of the active and reactive powers. Figs. 10(a) and (b) each show the active power and reference value of the active power and the reactive power and the reference value of the reactive power. For the active power reference value, it was changed from 0 kW to 27 kW at 0.4 sec and from 27 kW to 1 kW at 0.55 sec. For the reactive power reference value, it was changed from 2 to 26 kW at 0.45 sec and from 26 kW to 2 kW at 0.55 sec.

The waveforms of Fig. 10(a) are the waveforms of the active and reactive powers when the conventional MPDPC algorithm is used. The waveforms of Fig. 10(b) are the waveforms of the active and reactive powers when the proposed MPDPC is used. When performing the active and reactive power controls from the arbitrary initial point, it is verified that the mutual interference component is minimized in the transient interval where the reference value changes abruptly by using the proposed MPDPC.

Fig. 11 shows the simulation waveform for the case where the inductance value in control is different from the actual inductance value to verify the robustness of the proposed MPDPC. It shows simulation waveforms when the inductance values in control are -50% and 200%. The ripples of active and reactive powers increase and there will be some influence on power factor since a dc offset occurs on power due to the wrong inductance value. Through the simulation result,

This article has been accepted for publication in a future issue of this journal, but has not been fully edited. Content may change prior to final publication. Citation information: DOI 10.1109/TIE.2014.2352214, IEEE Transactions on Industrial Electronics

TABLE II
PARAMETERS FOR EXPERIMENT

Grid voltage (line-to-line)	380 Vac [rms]
DC-link voltage	700 Vdc
DC-link capacitor	3300 uF
Rated power	25 kW
Filter inductance	8 mH
Switching frequency	20 kHz

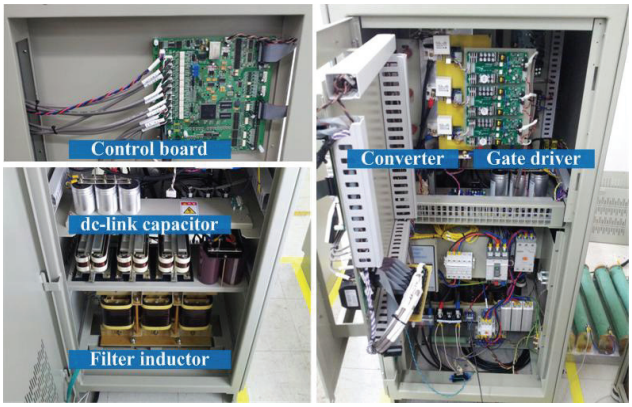

Fig. 12. Experimental setup of an AC/DC PWM converter.

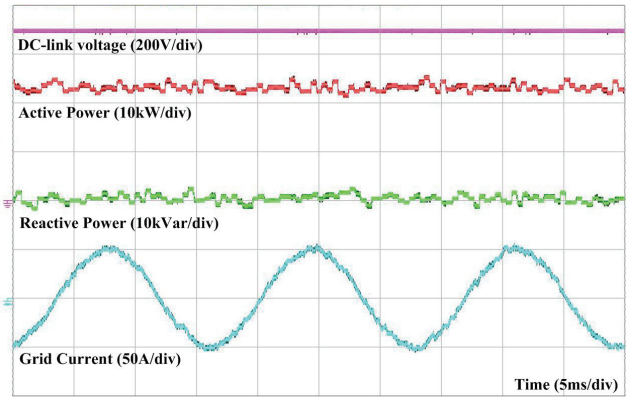

Fig. 13. Steady state response of the AC/DC PWM converter.

although the difference of the inductance value affects system performance of the proposed MPDPC, it is verified that the difference of the inductance, from -50% to 200%, does not affect the system stability.

V. EXPERIMENTAL RESULTS

The experiments are performed to verify the proposed control scheme. Fig. 12 shows the configuration of the experimental setup. It is composed into an IGBT based three-phase converter, switching at 20 kHz. The converter is connected to the grid through a filter inductor. The proposed method is programmed on a TMS320F28335 digital signal processor (DSP). The experiment conditions are performed under the conditions listed in Table II. The compensation waveforms between the proposed and conventional methods

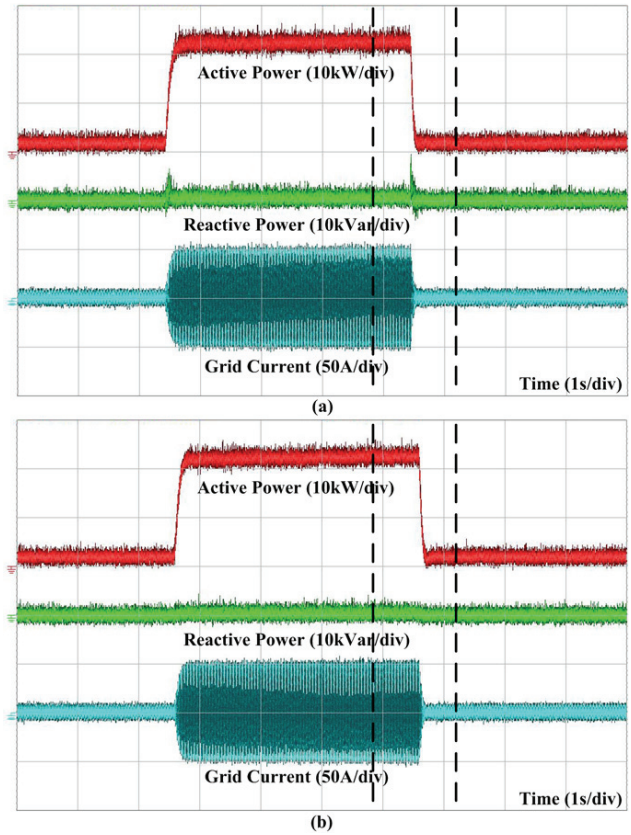

Fig. 14. Experimental results : step responses of active power.
(a) Conventional MPDPC. (b) Proposed MPDPC.

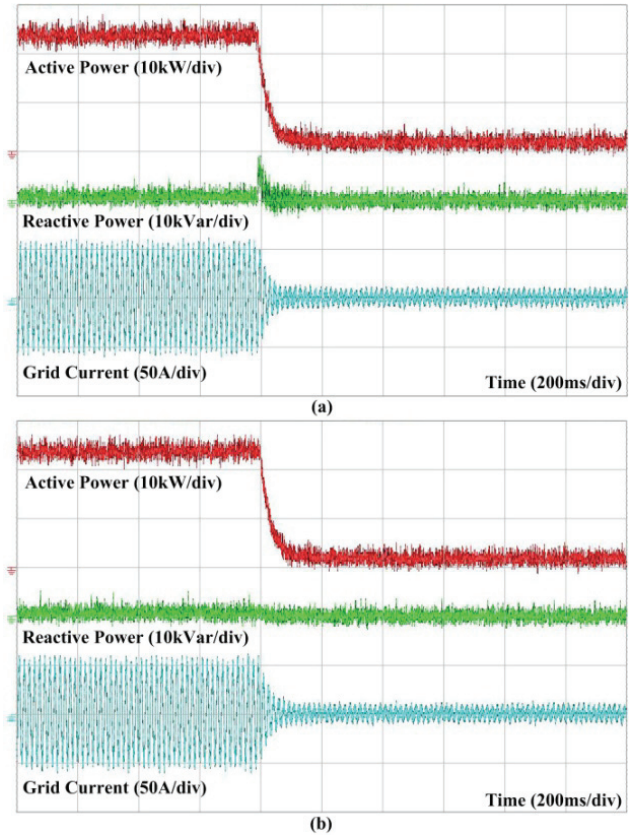

Fig. 15. Experimental results : expanded view of Fig. 14.
(a) Conventional MPDPC. (b) Proposed MPDPC.

This article has been accepted for publication in a future issue of this journal, but has not been fully edited. Content may change prior to final publication. Citation information: DOI 10.1109/TIE.2014.2352214, IEEE Transactions on Industrial Electronics

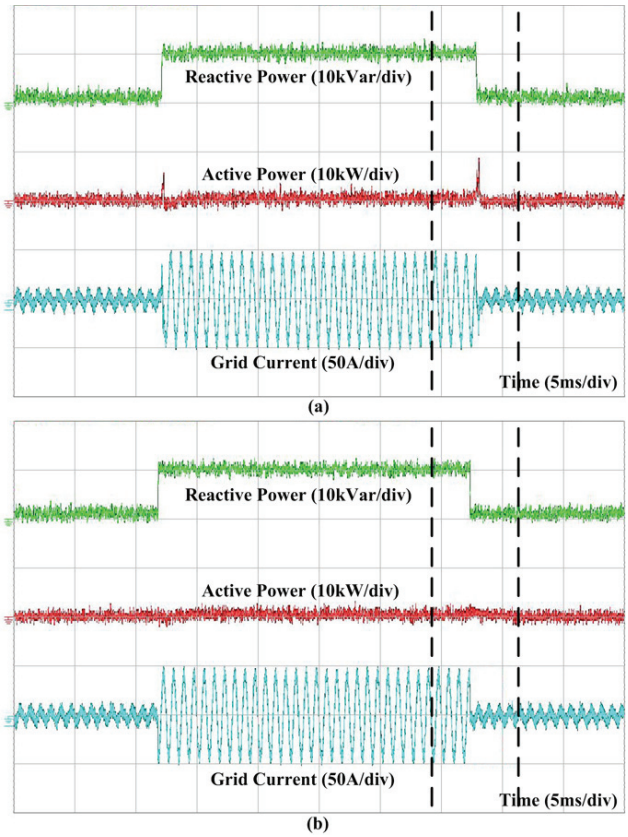

Fig. 16. Experimental results : step responses of reactive power.
(a) Conventional MPDPC. (b) Proposed MPDPC.

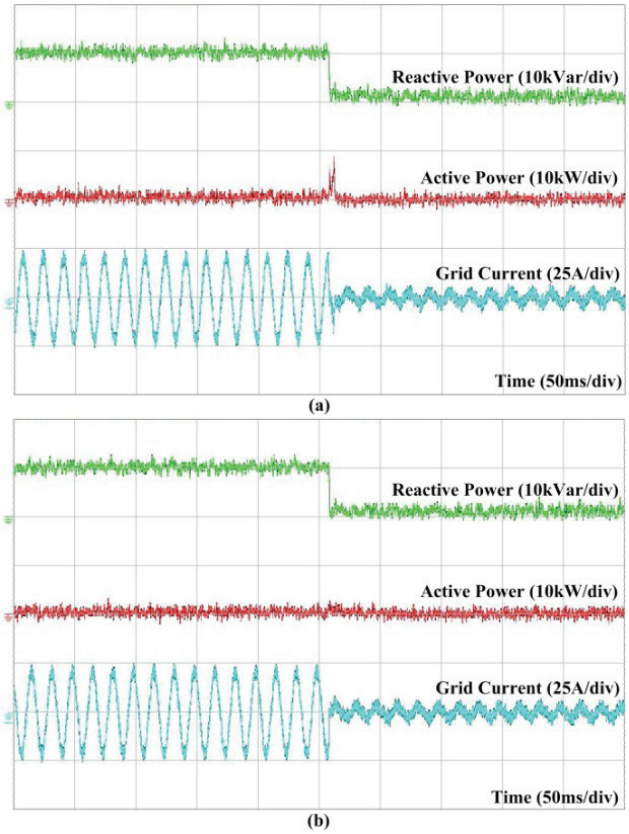

Fig. 17. Experimental results : expanded view of Fig. 16.
(a) Conventional MPDPC. (b) Proposed MPDPC.

are both performed under the same switching frequency of 20kHz.

Fig. 13 shows the waveform of the steady state when the converter is operated using the proposed MPDPC. From top, they are the dc-link voltage, active power, reactive power, and a-phase grid current. The dc-link voltage and the grid current are measured with the voltage and current probes, and the waveforms of reactive and active powers are viewed through the digital-to-analog (DA) function. It can be presented that the dc-link voltage is well maintained to the reference voltage of 700 V when the active power is generated at 23 kW. The input current has a nearly sinusoidal waveform.

Fig. 14 shows the experimental waveforms when the reactive power is controlled at 0 kVar and the active power is varied from 2 kW to 23 kW and then to 2 kW. From top, they show the active power, reactive power, and a-phase grid current. The sector where the mutual interference occurs is marked in dashed lines. Fig. 15 is the expanded view of the area between the dashed lines where the mutual interference occurs in Fig. 14. In the case of the MPDPC is performed using the conventional cost function, it can be seen that the mutual interference is generated on the reactive power side where the control weight is small among the control target in the sector where the reference of the active power changes like in Fig. 15(a). To improve the control performance of the converter, the MPDPC is performed through the reconfigured cost function. In the Fig. 15(b), it can be verified that the control performance is improved since the unstable sector generated by the mutual interference eliminated. In the case of performing the step change to the output load for the active power variation, the reference value of the active power is generated by the PI controller for the output voltage control. The transient response of the active power is influenced by the transient response of the output voltage controller.

Fig. 16 is the experimental waveforms for comparing the conventional MPDPC with the proposed MPDPC in the situation where the reactive power varies. The active power is controlled at 0 kW and the reactive power is varied from 2 kVar to 10 kVar and then to 2 kVar. Fig. 17 is the expanded view of the area between the dashed lines where the mutual interference occurs in Fig. 16. In the case of varying the reactive power, likewise changing the active power in Fig. 15(a), it can be seen through Fig. 17(a) that the mutual interference is generated when the MPDPC is performed by using the conventional cost function. To solve this problem, the proposed MPDPC is applied. The generated mutual interference in Fig. 17(a) is eliminated in Fig. 17(b) and the dynamic performance of the system is improved.

VI. Conclusion

This paper proposes the control scheme for the dynamic performance improvement for the AC/DC PWM converter using the MPDPC. The proposed method guarantees performance of the system even if the mutual interference occurs from the use of the conventional cost function. The cost function is reorganized to solve the mutual interference

problem generated by using the single cost function from the conventional MPDPC. Using the proposed method, the reduced dynamic performance of the system, caused by the mutual interference, has been enhanced and, thus, the performance of the system is improved. The validity of the proposed method was demonstrated by the simulations and experimental results.

REFERENCES

[1] M. Malinowski, M. P. Kazmierkowski, and A. M. Trzynadlowski, "A comparative study of control techniques for PWM rectifiers in ac adjustable speed drives," *IEEE Trans. Power Electron.*, vol. 18, no. 6, pp. 1390–1396, Nov. 2003.

[2] F. Blaabjerg, R. Teodorescu, M. Liserre, and A. Timbus, "Overview of control and grid synchronization for distributed power generation systems," *IEEE Trans. Ind. Electron.*, vol. 53, no. 5, pp. 1398–1409, Oct. 2006.

[3] B. Chen and G. Joos, "Direct power control of active filters with averaged switching frequency regulation," *IEEE Trans. Power Electron*., vol. 23, no. 6, pp. 2729–2737, Nov. 2008.

[4] Q. N. Trinh and H. H. Lee, "An Advanced Current Control Strategy for Three-Phase Shunt Active Power Filters," *IEEE Trans. Ind. Electron*., vol. 60, no. 12, pp. 5400–5410, Dec. 2013.

[5] X. Liu, P, C. Loh, P. Wang, and F. Blaabjerg, "A Direct Power Conversion Topology for Grid Integration of Hybrid AC/DC Energy Resources," *IEEE Trans. Ind. Electron.*, vol. 60, no. 12, pp. 5696–5707, Dec. 2013.

[6] J. Alonso-Martinez, J. E. Carrasco, and S. Arnaltes, "Table-based direct power control: A critical review for microgrid applications," *IEEE Trans. Power Electron.*, vol. 25, no. 12, pp. 2949–2961, Dec. 2010.

[7] J. Rodriguez, J. Dixon, J. Espinoza, J. Pontt, and P. Lezana, "PWM regenerative rectifiers: State of the art," *IEEE Trans. Ind. Electron.*, vol. 52, no. 1, pp. 5–22, Feb. 2005.

[8] D. S. Wijeratne and G., Moschopoulos, "A Three-Phase Single-Stage AC–DC PWM Buck-Type Full-Bridge Converter: Analysis, Design, and Characteristics," *IEEE Trans. Ind. Electron*., vol. 60, no. 10, pp. 4201–4214, Oct. 2013.

[9] J. H. Kim, S. T. Jou, D. K. Choi, and K. B. Lee, "Direct Power Control of Three-Phase Boost Rectifiers Using a Sliding-Mode Scheme," *Journal of Power Electronics*, vol. 13, no. 6, pp. 1000-1007, Nov. 2013.

[10] J. Dai, D. Xu, B.Wu, and N. R. Zargari, "Unified DC-link current control for low-voltage ride-through in current-source-converter-based wind energy conversion systems," *IEEE Trans. Power Electron.*, vol. 26, no. 1, Jan. 2011.

[11] J. Dai, D. D. Xu, and B.Wu, "A novel control scheme for current-source converter-based PMSG wind energy conversion systems," *IEEE Trans. Power Electron*., vol. 24, no. 4, pp. 963–972, Apr. 2009.

[12] J. R. Rodriguez, J. W. Dixon, J. R. Esponoza, J. Pontt, and P. Lezana, "PWM regenerative rectifiers: State of the art," *IEEE Trans. Ind. Electron.*, vol. 52, no. 1, pp. 5–22, Feb. 2005.

[13] Y.W. Li, M. Pande, N. Zargari, and B.Wu, "An input power factor control strategy for high-power current-source induction motor drive with active front-end," *IEEE Trans. Power Electron*., vol. 25, no. 2, pp. 352–359, Feb. 2010.

[14] S. Kwak and H. A. Toliyat, "Design and rating comparisons of PWM voltage source rectifiers and active power filters for AC drives with unity power factor," *IEEE Trans. Power Electron*., vol. 20, no. 5, pp. 1133–1142, Sep. 2005.

[15] T. G. Habetler, "A space vector-based rectifier regulator for AC/DC/AC converters," *IEEE Trans. Power Electron*., vol. 8, no. 1, pp. 30–36, Jan. 1993.

[16] M. P. Kazmierowski, M. Jasinski, and G. Wrona, "DSP-based control of grid-connected power converters operating under grid distortions," *IEEE Trans. Ind. Informat*., vol. 7, no. 2, pp. 204–211, May 2011.

[17] A. Bouafia, J.-P. Gaubert, and F. Krim, "Predictive direct power control of three-phase pulsewidth modulation (PWM) rectifier using space-vector modulation (SVM)," *IEEE Trans. Power Electron*., vol. 25, no. 1, pp. 228–236, Jan. 2010.

[18] J. Hu, L. Shang, Y. He, and Z. Z. Zhu., "Direct active and reactive power regulation of grid-connected DC/AC converters using sliding mode control approach," *IEEE Trans. Power Electron*., vol. 26, no. 1, pp. 210–222, Jan. 2011.

[19] V. Blasko and V. Kaura, "A new mathematical model and control of a three-phase ac-dc voltage source converter," *IEEE Trans. Power Electron.*, vol. 12, no. 1, pp. 116–123, Jan. 1997.

[20] T. Noguchi, H. Tomiki, S. Kondo, and I. Takahashi, "Direct power control of PWM converter without power-source voltage sensors," *IEEE Trans. Ind. Appl.*, vol. 34, no. 3, pp. 473–479, May/Jun. 1998.

[21] S. Mathapati and J. Bocker, "Analytical and Offline Approach to Select Optimal Hysteresis Bands of DTC for PMSM," *IEEE Trans. Ind. Electron.*, vol. 60, no. 3, pp. 885–895, Mar. 2013.

[22] Y. Zhang and J. Zhu, "Direct torque control of permanent magnet synchronous motor with reduced torque ripple and commutation frequency," *IEEE Trans. Power Electron.*, vol. 26, no. 1, pp. 235–248, Jan. 2011.

[23] G. Escobar, A. Stankovic, J. Carrasco, E. Galvan, and R. Ortega, "Analysis and design of direct power control (DPC) for a three phase synchronous rectifier via output regulation subspaces," *IEEE Trans. Power Electron.*, vol. 18, no. 3, pp. 823–830, May 2003.

[24] A. Bouafia, J.-P. Gaubert, and F. Krim, "Analysis and design of new switching table for direct power control of three-phase PWM rectifier," in Proc. *13th Power Electron. Motion Control Conf*., 2008, pp. 703–709.

[25] A. Bouafia, F. Krim, and J.-P. Gaubert, "Fuzzy-logic-based switching state selection for direct power control of three-phase PWM rectifier," *IEEE Trans. Ind. Electron.*, vol. 56, no. 6, pp. 1984–1992, Jun. 2009.

[26] S. Muller, U. Ammann, and S. Rees, "New time-discrete modulation scheme for matrix converters," *IEEE Trans. Ind. Electron.*, vol. 52, no. 6, pp. 1607–1615, Dec. 2005.

[27] P. Cortes, J. Rodriguez, C. Silva, and A. Flores, "Delay compensation in model predictive current control of a three-phase inverter," *IEEE Trans. Ind. Electron.*, vol. 59, no. 2, pp. 1323-1325, Feb. 2012.

[28] F. Villarroel, J. R. Espinoza, C. A. Rojas, J. Rodriguez, M. Rivera, and D. Sbarbaro, "Multiobjective switching state selector for finite-states model predictive control based on fuzzy decision making in a matrix converter," *IEEE Trans. Ind. Electron.*, vol. 60, no. 2, pp. 589–599, Feb. 2013.

[29] M. Rivera, A. Wilson, C. A. Rojas, J. Rodríguez, J. R. Espinoza, P. W. Wheeler, and L. Empringham, "A comparative assessment of model predictive current control and space vector modulation in a direct matrix converter," *IEEE Trans. Ind. Electron.*, vol. 60, no. 2, pp. 578–588, Feb. 2013.

[30] H. Guzman, M. J. Duran, F. Barrero, B. Bogado, and S. Toral, "Speed Control of Five-Phase Induction Motors With Integrated Open-Phase Fault Operation Using Model-Based Predictive Current Control Techniques," *IEEE Trans. Ind. Electron.*, vol. 61, no. 9, pp. 4474–4484, Sept. 2014.

[31] C. S. Lim, E. Levi, M. Jones, N. A. Rahim, W. P. Hew, "FCS-MPC-Based Current Control of a Five-Phase Induction Motor and its Comparison with PI-PWM Control," *IEEE Trans. Ind. Electron.*, vol. 61, no. 1, pp. 149-163, Jan. 2014.

[32] J. Rodriguez, J. Pontt, C. Silva, P. Correa, P. Lezana, P. Cortes, and U. Ammann, "Predictive current control of a voltage source inverter," *IEEE Trans. Ind. Electron.*, vol. 54, no. 1, pp. 495–503, Feb. 2007.

[33] J. Rodríguez, J. Pontt, C. Silva, M. Salgado, S. Rees, U. Ammann, P. Lezana, R. Huerta, and P. Cortés, "Predictive control of a three-phase inverter," *IEE Electronics Letters*, vol. 40, no. 9, pp. 561–562, Apr. 29, 2004.

[34] E. Lee, K. B. Lee, Y. Lee, and J. Song, "High Performance Current Controller for Sparse Matrix Converter Based on Model Predictive Control," *Journal of Electrical Engineering & Technology*, vol. 8, no. 5, pp. 1138-1145, Sept. 2013.

[35] V. Yaramasu, M. Rivera, M. Narimani, B. Wu, J. Rodriguez, "Model Predictive Approach for a Simple and Effective Load Voltage Control of Four-Leg Inverter With an Output LC Filter," *IEEE Trans. Ind. Electron.*, vol. 61, no. 10, pp. 5259-5270, Oct. 2014.

[36] C. S. Lim, E. Levi, M. Jones, N. A. Rahim, W. P. Hew, "A Comparative Study of Synchronous Current Control Schemes Based on FCS-MPC and PI-PWM for a Two-Motor Three-Phase Drive," *IEEE Trans. Ind. Electron.*, vol. 61, no. 8, pp. 3867-3878, Aug. 2014.

[37] C. A. Rojas, J. Rodriguez, F. Villarroel, J. R. Espinoza, C. A. Silva, M. Trincado, "Predictive Torque and Flux Control Without Weighting Factors," *IEEE Trans. Ind. Electron.*, vol. 60, no. 2, pp. 681-690, Feb. 2013.

[38] Z. Song; C. Xia; T. Liu, "Predictive Current Control of Three-Phase Grid-Connected Converters With Constant Switching Frequency for Wind Energy Systems," *IEEE Trans. Ind. Electron.*, vol. 60, no. 6, pp. 2451-2464, Jun. 2013.

[39] M. A. Perez, J. Rodriguez, E. J. Fuentes, F. Kammerer, "Predictive Control of AC–AC Modular Multilevel Converters," *IEEE Trans. Ind. Electron.*, vol. 59, no. 7, pp. 2832-2839, Jul. 2012.

[40] P. Cortes, J. Rodriguez, D. E. Quevedo, and C. Silva, "Predictive current control strategy with imposed load current spectrum," *IEEE Trans. Power Electron.*, vol. 23, no. 2, pp. 612–618, Mar. 2008.

[41] R. Vargas, P. Cortes, U. Ammann, J. Rodriguez, and J. Pontt, "Predictive control of a three-phase neutral-point-clamped inverter," *IEEE Trans. Ind. Electron.*, vol. 54, no. 5, pp. 2697–2705, Oct. 2007.

[42] P. Cortes, J. Rodriguez, P. Antoniewicz, and M. Kazmierkowski, "Direct power control of an AFE using predictive control," *IEEE Trans. Power Electron.*, vol. 23, no. 5, pp. 2516–2523, Sep. 2008.

[43] D. E. Quevedo, R. P. Aguilera, M. A. Perez, P. Cortes, and R. Lizana, "Model Predictive Control of an AFE Rectifier With Dynamic References", *IEEE Trans. Power Electron*., vol. 27 , no. 7, pp. 3128-3136, Jul. 2012.

[44] Y. Zhang, W. Xie, and Z. Li, "Model Predictive Direct Power Control of a PWM Rectifier With Duty Cycle Optimization," *IEEE Trans. Power Electron.*, vol. 28, no. 11, pp. 5343–5351, Nov. 2013.

[45] P. Cortes, J. Rodriguez, C. Silva, and A. Flores, "Delay compensation in model predictive current control of a three-phase inverter," *IEEE Trans. Ind. Electron*., vol. 59, no. 2, pp. 1323–1325, Feb. 2012.

Dae-Keun Choi was born in Seoul, Korea, in 1980. He received the B.S. and M.S. degrees in Electronic Engineering from the Ajou University, Korea, in 2009 and 2011, respectively.

He is currently working toward the Ph.D. degree at Ajou University, Korea. His research interests include power conversion and grid-connected systems

Kyo-Beum Lee (S'02-M'04-SM'10) was born in Seoul, Korea, in 1972. He received the B.S. and M.S. degrees in electrical and electronic engineering from the Ajou University, Korea, in 1997 and 1999, respectively.

He received the Ph.D. degree in electrical engineering from the Korea University, Korea in 2003. From 2003 to 2006, he was with the Institute of Energy Technology, Aalborg University, Aalborg, Denmark. From 2006 to 2007, he was with the Division of Electronics and Information Engineering, Chonbuk National University, Jeonju, Korea. In 2007 he joined the School of Electrical and Computer Engineering, Ajou University, Suwon, Korea. His research interests include electric machine drives, electric vehicles, and renewable power generations.